ISSN: 2458-8989

Natural and Engineering Sciences

NESciences, 2026, 11 (3): 802-812 doi: 10.28978/nesciences.263063

Age-Dependent Morphometric and Immunohistochemical Remodeling of the Rat Spleen and Thymus Following Mycobacterial Antigen Stimulation: Digital Image-Assisted Analysis

Teshaev Shukhrat Jumayevich[1], Toirov Oybek Aliyevich[2], Khasanov Aziz Qosimovich[3], Umarov Zafarbek Zaripboyevich[4], Egamberdiyev Kuvonchbek Kosimovich[5], Rakhimov Anvar Pulatboevich[6]

[1] Doctor of Medical Sciences, Professor, Department of Anatomy, Clinical Anatomy and Operative Surgery with Topographic Anatomy, Bukhara State Medical Institute named after Abu Ali ibn Sino, Bukhara, Uzbekistan. Email: teshayev@bsmi.uz, ORCID: 0009-0002-1996-4275

[2] PhD, Surgeon, Department of Vascular Surgery, Republican Specialized Scientific and Practical Medical Center of Surgery named after Academician V. V. Vakhidov, Tashkent, Uzbekistan. Email: Oybektoirov6@mail.com, ORCID: 0009-0002-6229-8247

[3] PhD, Associate Professor, Department of General Surgery, Bukhara State Medical Institute named after Abu Ali ibn Sino, Bukhara, Uzbekistan. Email: xasanovaq@gmail.com, ORCID: 0000-0003-4430-6522

[4] Doctor of Philosophy (PhD) in Medical Sciences, MD, General Surgeon, Senior Lecturer, Department of Surgical Diseases and Transplantology, Urgench State Medical Institute (formerly Urgench Branch of Tashkent Medical Academy), Urgench, Uzbekistan. Email: doctor_uzz1986@mail.ru, ORCID: 0009-0002-6298-9144

[5] Doctor of Philosophy (PhD) in Medical Sciences, Associate Professor, Department of Clinical Sciences, Mamun University, Khorezm, Uzbekistan. Email: kuvonch8484@mail.ru, ORCID: 0009-0009-1516-0684

[6] Doctor of Philosophy (PhD) in Medical Sciences, MD, Associate Professor, Department of Surgical Diseases and Transplantology, Urgench State Medical Institute (formerly Urgench Branch of Tashkent Medical Academy), Urgench, Uzbekistan. Email: anvar_2277@mail.ru, ORCID: 0009-0007-1800-5503

Abstract

Background: The spleen and thymus undergo age-related remodeling and respond to immune stimulation. Combining conventional histology, morphometry, and immunohistochemistry can provide a quantitative description of these changes.
Objective: To characterize age-dependent morphometric, stromal, and immunohistochemical changes in the spleen and thymus of rats following experimental stimulation with a mycobacterial antigen-containing adjuvant.
Materials and Methods: Spleen and thymus tissues from 4- and 9-month-old male outbred rats were examined in age-matched control and experimental conditions. Sections were evaluated using hematoxylin and eosin and Van Gieson staining. Digital image analysis was performed with QuPath v0.5.1. Splenic measurements included white- and red-pulp proportions, lymphoid follicle diameter,

*Corresponding Author: Teshaev Shukhrat Jumayevich, E-mail: teshayev@bsmi.uz

periarteriolar lymphoid sheath thickness, and central artery diameter. Thymic measurements included cortical and medullary proportions, the corticomedullary ratio, thymocyte density, Hassall's corpuscle diameter, and collagen-positive area. Splenic CD3, CD20, and CD68 and thymic CD138 and caspase-3 reactions were assessed.

Results: At 4 months, the splenic white-pulp proportion increased from 32.8 ± 1.2% in controls to 41.9 ± 1.5% in the experimental group; at 9 months, it increased from 30.5 ± 1.1% to 44.8 ± 1.6%. In the 9-month thymus, the cortical proportion decreased from 61.7 ± 1.7% to 48.5 ± 1.5%, while the medullary proportion increased from 38.3 ± 1.7% to 51.5 ± 1.5%. The corticomedullary ratio fell from 1.61 ± 0.07 to 0.94 ± 0.05, thymocyte density from 10,980 ± 360 to 8,240 ± 310 cells/mm², and Hassall's corpuscle diameter increased from 45.3 ± 1.6 to 67.5 ± 2.3 μm. Collagen-positive area increased in both organs. Reported splenic CD3- and CD20-associated percentages decreased, whereas CD68-associated percentages increased. The available thymic immunohistochemical records did not permit a reliable age-matched quantitative comparison.

Conclusion: Experimental mycobacterial-antigen stimulation was associated with age-dependent remodeling of splenic lymphoid compartments and thymic cortical-medullary organization, accompanied by increased collagen-positive area and altered immunohistochemical marker patterns. Digital image-assisted morphometry provided quantitative descriptions of these changes. The findings should be interpreted in light of the experimental model and the need to verify subgroup sizes and the denominators used for immunohistochemical percentages.

Keywords: Spleen; thymus; mycobacterial antigen; digital morphometry; immunohistochemistry.

Available Online: 10/09/2026

Introduction

The immune system depends on the coordinated activity of primary and secondary lymphoid organs, which provide the structural and cellular environment required for lymphocyte development, antigen recognition, and the initiation of immune responses. Among these organs, the thymus and spleen have complementary but distinct functions. The thymus is responsible for T-lymphocyte differentiation and selection, whereas the spleen contributes to systemic immune surveillance, antigen processing, and the organization of lymphocyte-mediated responses. Because their functions depend on specialized tissue architecture, changes in the proportions, dimensions, and cellular composition of their structural compartments may reflect alterations in immune homeostasis under experimental or pathological conditions [1,2].

The thymus has a characteristic organization consisting of cortical and medullary compartments. The cortex contains a high density of developing thymocytes, while the medulla supports later stages of T-cell maturation and mechanisms involved in the establishment of immunological tolerance. The relative proportions of these compartments, the density of thymocytes, and the structural characteristics of Hassall's corpuscles are therefore important morphometric indicators of thymic organization. Age-associated thymic involution is characterized by progressive changes in thymic architecture, including cortical reduction and an increase in the relative contribution of medullary and stromal components. Quantitative assessment of these features is essential for distinguishing age-related variation from changes associated with experimental stimulation or pathological processes [1,3].

The spleen is organized into white pulp, red pulp, and specialized marginal regions that facilitate interactions between circulating antigens, antigen-presenting cells, and lymphocyte populations. The white pulp contains T-cell-rich periarteriolar lymphoid sheaths and B-cell-associated lymphoid follicles, whereas the red pulp participates in blood filtration and the removal of aged or damaged blood cells. Consequently, measurements of white and red pulp proportions, lymphoid follicle diameter, periarteriolar lymphoid sheath thickness, and central artery diameter provide complementary information about splenic tissue organization. Changes in these parameters may indicate remodeling of lymphoid compartments, vascular alterations, or shifts in the relative distribution of immune-cell populations. However, morphometric findings should be interpreted together with histological and immunohistochemical observations rather than being considered independent evidence of a particular immune mechanism [2,4].

Experimental mycobacterial stimulation provides a model for investigating structural responses of lymphoid organs to an immunological challenge. Mycobacteria and their associated antigens can activate innate and adaptive immune pathways, involving antigen-presenting cells, macrophages, and lymphocyte populations. The resulting tissue response may differ between organs because the thymus

and spleen have different functional roles and microanatomical organizations. Furthermore, age may influence the magnitude and pattern of these responses. Comparative assessment of younger and older experimental animals can therefore help identify whether changes in lymphoid tissue architecture are associated with age, experimental stimulation, or an interaction between these factors. Such comparisons require clearly defined experimental groups and appropriate statistical analysis to avoid attributing age-related differences exclusively to the experimental intervention [1,2,4].

Conventional histological examination remains fundamental to the evaluation of tissue organization, cellular distribution, and structural injury. Nevertheless, qualitative microscopy alone may not fully capture subtle differences in tissue area, compartment proportions, cellular density, or the dimensions of individual structures. Manual measurements can also be time-consuming and may be affected by observer-related variability, sampling procedures, and differences in the selection of microscopic fields. Quantitative morphometry addresses these limitations by converting visible tissue characteristics into measurable variables, including area fractions, linear dimensions, ratios, and cell counts. These measurements facilitate comparisons between experimental groups and provide a quantitative basis for describing morphological changes [10,13,16,17].

Digital image analysis extends conventional morphometry by enabling the measurement of histological structures directly from digitized microscopic images. Depending on the software and analytical procedure, digital workflows may support image calibration, region selection, compartment delineation, measurement of tissue areas, cell counting, and quantification of staining intensity. When applied using standardized acquisition and analysis procedures, these methods can improve the consistency and reproducibility of quantitative tissue assessment. However, the reliability of digital measurements depends on image quality, stain consistency, spatial calibration, appropriate identification of tissue regions, and transparent reporting of the analytical workflow. Digital analysis should therefore be considered a measurement approach whose validity must be demonstrated for the parameters under investigation, rather than an automatic guarantee of accuracy [5–7].

The development of digital pathology and computational image analysis has also expanded opportunities for quantitative assessment of immunohistochemical markers. Immunohistochemistry provides information about the distribution of selected cellular or molecular markers within the histological context. In lymphoid tissues, CD3 can be used to identify T-cell-associated populations, while CD20 is commonly used to assess B-cell-associated populations. CD68 is frequently applied as a macrophage-associated marker. In the present study, these markers are relevant to the evaluation of splenic cellular composition. In the thymus, CD138 and caspase-3 provide additional immunohistochemical information, although interpretation must account for the biological specificity and limitations of each marker. Marker positivity alone does not establish the complete functional state of a cell population; consequently, immunohistochemical findings should be interpreted in relation to tissue morphology, staining protocols, and the method used to quantify positive reactions [7–9].

Recent advances in computational pathology have demonstrated the potential of image-analysis algorithms and deep-learning methods to quantify tissue compartments and improve the reproducibility of histopathological assessments. For example, a deep-learning approach developed for rat spleen sections was evaluated for identifying lymphoid compartments from hematoxylin-and-eosin-stained images, with immunohistochemical staining used to establish reference annotations [18]. Such studies demonstrate the potential of computational methods for research in lymphoid-organ morphology. At the same time, an important distinction must be maintained between conventional digital morphometry, software-assisted image analysis, and a validated artificial-intelligence model. The latter requires documented model architecture, training and validation procedures, reference annotations, and appropriate performance metrics. Accordingly, the use of digital image analysis in a morphological study should not automatically be described as the development or validation of an artificial-intelligence diagnostic system.

Our previous work published in Natural and Engineering Sciences examined morphometric and histological alterations in the spleen following chronic carbon monoxide exposure and assessed the corrective effects of Gulimaxsar [20]. This publication provides a relevant background for the quantitative evaluation of splenic tissue responses to experimental exposure. In addition, research published in the same journal has examined myocardial remodeling through an integrated approach incorporating morphometry, histopathology, and immunohistochemistry in an experimental rat model [21]. Together, these studies illustrate the relevance of combining structural measurements with tissue-based biomarker assessment in experimental morphology. However, the organs, experimental exposures, and biological mechanisms investigated in those publications differ from those addressed in

the present study; therefore, their findings should be regarded as methodological and thematic context rather than direct evidence of the effects of mycobacterial stimulation.

Despite progress in quantitative histopathology, the combined assessment of age-dependent splenic and thymic remodeling under experimental mycobacterial stimulation remains an important area for investigation. Evaluating both organs within the same experimental framework allows their structural responses to be compared using a consistent set of morphometric and immunohistochemical procedures. Such an approach may reveal differences in the relative proportions of lymphoid compartments, the distribution of selected immune-cell-associated markers, and the extent of stromal remodeling. Nevertheless, the interpretation of these differences requires careful consideration of age-matched controls, the characteristics of the experimental model, sample size, and the statistical significance of observed changes.

Therefore, the aim of this study was to characterize age-dependent morphometric, stromal, and immunohistochemical changes in the spleen and thymus of rats following experimental mycobacterial stimulation using quantitative, image-assisted analysis. The assessment included splenic white and red pulp proportions, lymphoid follicle diameter, periarteriolar lymphoid sheath thickness, and central artery diameter, together with thymic cortical and medullary proportions, the corticomedullary ratio, thymocyte density, and Hassall's corpuscle diameter. Collagen content and selected immunohistochemical markers were also considered to provide complementary information on tissue remodeling. By integrating these measurements, the study sought to provide a quantitative description of structural changes in two functionally distinct lymphoid organs and to compare the observed patterns between 4- and 9-month-old animals.

Materials and Methods

2.1. Study Design and Experimental Animals

The experimental model used Complete Freund's Adjuvant (CFA) containing heat-inactivated Mycobacterium tuberculosis H37Ra. The adjuvant was administered once to animals initially aged 3 or 8 months, followed by a one-month observation period; tissue endpoints were assessed at 4 and 9 months, respectively. Animals underwent a 7–10-day acclimatization period before the experiment.

2.2. Tissue Sampling and Histological Examination

Spleen and thymus tissues were collected at the end of the observation period. The dissertation reports fixation in 10% neutral buffered formalin for 24–48 hours, followed by routine histological processing. Sections were stained with hematoxylin and eosin for general tissue architecture and Van Gieson stain for collagen-containing stromal components.

Splenic measurements included white- and red-pulp proportions, lymphoid follicle diameter, periarteriolar lymphoid sheath (PALS) thickness, and central artery diameter. Thymic measurements included cortical and medullary area proportions, the corticomedullary ratio, thymocyte density, and Hassall's corpuscle diameter.

2.3. Immunohistochemical Assessment

Immunohistochemical assessment included CD3, CD20, and CD68 in the spleen and CD138 and caspase-3 in the thymus. DAB was used as the chromogen, and representative slides were examined at ×200 magnification. The dissertation reports digital assessment using QuPath v0.5.1. The biological interpretation of marker positivity was restricted to the marker-associated cellular patterns; marker positivity alone was not treated as proof of a complete functional state.

2.4. Digital Morphometric Analysis

Digital morphometry was used to quantify tissue-compartment proportions, linear dimensions, cell density, and collagen-positive area. Immunohistochemical images were assessed with QuPath v0.5.1. The analysis should be reported as software-assisted digital image analysis; the manuscript does not establish that a validated artificial-intelligence model was trained or tested.

2.5. Statistical Analysis

The dissertation reports quantitative data as mean ± standard error (M ± m). It describes Shapiro–Wilk testing for normality, Student's t-test or Mann–Whitney U test for two-group comparisons, ANOVA or Kruskal–Wallis testing for comparisons involving multiple groups, and Spearman correlation where relevant. The stated significance threshold was $p < 0.05$.

Results

3.1. Age-dependent changes in splenic architecture

The dissertation data indicate that mycobacterial stimulation was associated with redistribution of splenic tissue compartments and enlargement of selected lymphoid and vascular structures in both age

groups. In 4-month-old animals, the white pulp proportion increased from 32.8 ± 1.2% in controls to 41.9 ± 1.5% in the experimental group, whereas the red pulp proportion decreased from 67.2 ± 1.2% to 58.1 ± 1.5%. The lymphoid follicle diameter increased from 286.4 ± 9.8 μm to 341.6 ± 11.2 μm, and periarteriolar lymphoid sheath (PALS) thickness increased from 47.8 ± 1.9 μm to 56.5 ± 2.2 μm. Central artery diameter increased from 39.6 ± 1.5 μm to 46.8 ± 1.8 μm.

In 9-month-old animals, the differences between the age-matched control and experimental groups were more pronounced for several parameters. White pulp increased from 30.5 ± 1.1% to 44.8 ± 1.6%, while red pulp decreased from 69.5 ± 1.1% to 55.2 ± 1.6%. Lymphoid follicle diameter increased from 273.7 ± 10.1 μm to 365.8 ± 12.6 μm, PALS thickness from 44.6 ± 1.8 μm to 61.2 ± 2.4 μm, and central artery diameter from 41.5 ± 1.7 μm to 51.9 ± 2.0 μm.

Taken together, these measurements describe a shift toward a larger relative white-pulp compartment, enlarged lymphoid follicles, thicker periarteriolar lymphoid sheaths, and larger central arteries after experimental stimulation. These are descriptive comparisons of reported group means; statistical significance should be stated only after confirming the corresponding tests and p-values in the original tables.

Figure 1. Age-stratified comparison of splenic morphometric parameters between control and experimental groups. Error bars represent the reported ± values.

Table 1. Splenic morphometric parameters in control and experimental groups

Parameter	Age	Control	Experimental	Reported change
White pulp (%)	4 months	32.8 ± 1.2	41.9 ± 1.5	+27.7%
Red pulp (%)	4 months	67.2 ± 1.2	58.1 ± 1.5	−13.5%
Lymphoid follicle diameter (μm)	4 months	286.4 ± 9.8	341.6 ± 11.2	+19.3%
PALS thickness (μm)	4 months	47.8 ± 1.9	56.5 ± 2.2	+18.2%
Central artery diameter (μm)	4 months	39.6 ± 1.5	46.8 ± 1.8	+18.2%
White pulp (%)	9 months	30.5 ± 1.1	44.8 ± 1.6	+46.9%
Red pulp (%)	9 months	69.5 ± 1.1	55.2 ± 1.6	−20.6%
Lymphoid follicle diameter (μm)	9 months	273.7 ± 10.1	365.8 ± 12.6	+33.7%
PALS thickness (μm)	9 months	44.6 ± 1.8	61.2 ± 2.4	+37.2%
Central artery diameter (μm)	9 months	41.5 ± 1.7	51.9 ± 2.0	+25.1%

3.2. Changes in splenic collagen content

Collagen-positive area increased in the spleen in both age groups. At 4 months, the reported value rose from 10.7% in controls to 21.7% in the experimental group (approximately 2.03-fold); at 9 months, it rose from 11.2% to 20.8% (approximately 1.86-fold). These measurements indicate a greater collagen-

positive area after experimental stimulation. The percentage alone does not describe collagen distribution or fibre organization, which should also be assessed histologically.

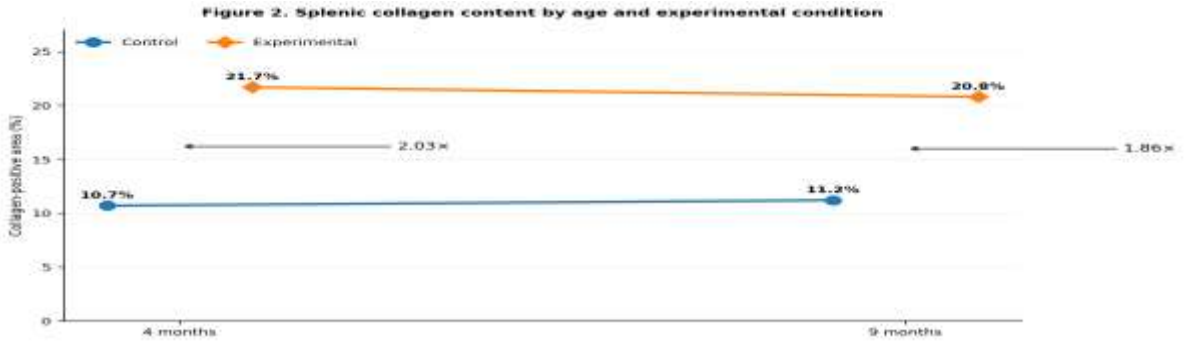

Figure 2. Splenic collagen-positive area in control and experimental groups. Fold changes are calculated from the reported percentages

Age	Control (%)	Experimental (%)	Experimental/control
4 months	10.7	21.7	2.03×
9 months	11.2	20.8	1.86×

3.3. Immunohistochemical profile of the spleen

The reported splenic immunohistochemical percentages showed different patterns across the three markers. At 4 months, CD3-associated values decreased from 30.57% in controls to 10.19% in the experimental group, and CD20-associated values decreased from 26.11% to 9.75%; CD68-associated values increased from 9.72% to 27.54%. At 9 months, CD3 decreased from 38.10% to 16.11%, CD20 from 32.74% to 7.97%, while CD68 increased from 7.27% to 26.18%. These values describe a lower proportion of CD3- and CD20-associated reactions and a higher CD68-associated proportion in the

experimental groups. The percentages are interpreted descriptively because the scoring denominator and aggregation level are not available.

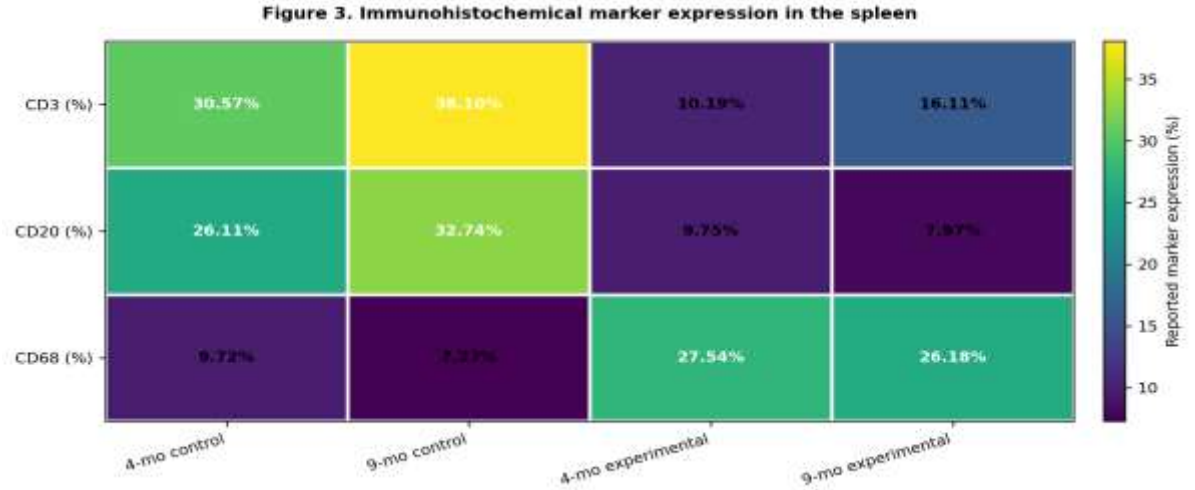

Figure 3. Heatmap of reported splenic immunohistochemical marker expression across age and experimental condition.

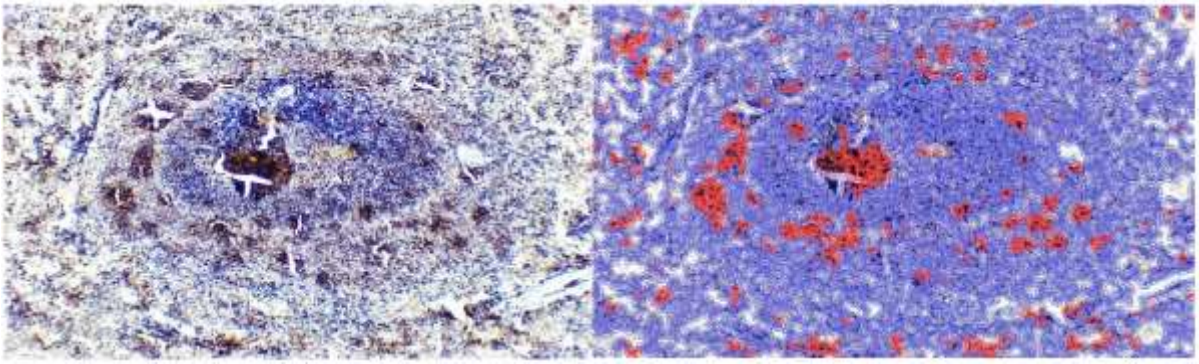

Figure 4. Immunohistochemical detection of CD68-positive cells in the spleen of 4-month-old control rats. The tissue was stained using the DAB chromogen method and examined at ×200 magnification.

The right panel shows the QuPath-based digital analysis, with CD68-positive cells highlighted in red. A total of 3,377 cells were analyzed, of which 327 were positive for CD68 (9.72%). The analyzed tissue area was 671,048 px².

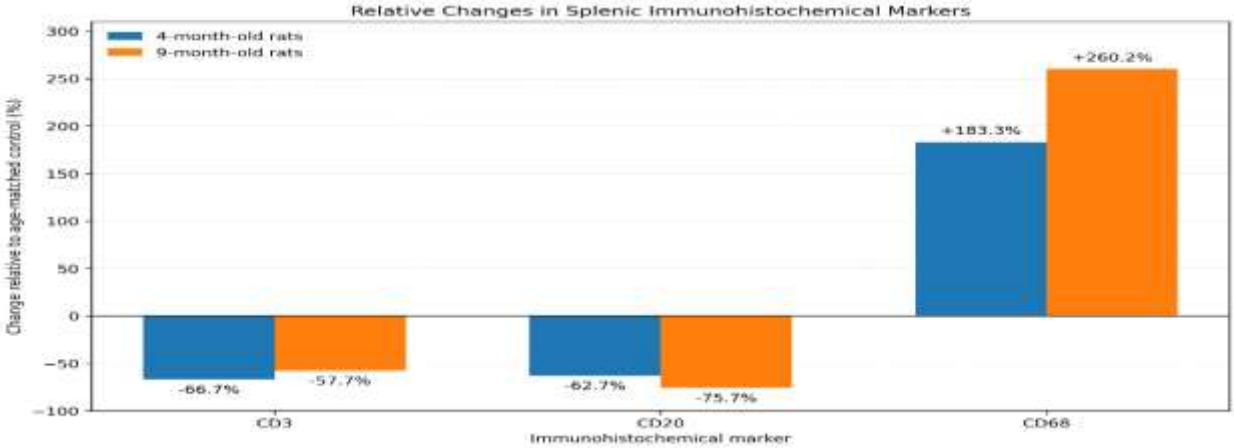

Figure 5. Relative changes in reported splenic immunohistochemical marker values in experimental rats compared with age-matched controls. Percentage changes were calculated for CD3, CD20,

and CD68 using the corresponding control-group values as references. Negative values indicate decreases, whereas positive values indicate increases relative to age-matched controls. These values represent descriptive percentage changes and do not independently establish statistical significance.

Table 2. Reported immunohistochemical marker values in the spleen of control and experimental rats at 4 and 9 months of age

Marker	4-month control	4-month experimental	9-month control	9-month experimental
CD3 (%)	30.57	10.19	38.10	16.11
CD20 (%)	26.11	9.75	32.74	7.97
CD68 (%)	9.72	27.54	7.27	26.18

Note: Values are presented as reported in the source dataset.

3.4. Age-dependent morphometric changes in the thymus

Thymic morphometry showed both age-associated differences in the control animals and more pronounced changes after experimental stimulation. At 4 months, the cortical area proportion decreased from 68.4 ± 1.8% in controls to 59.2 ± 1.6% in the experimental group, while the medullary proportion increased from 31.6 ± 1.8% to 40.8 ± 1.6%. The corticomedullary ratio declined from 2.16 ± 0.08 to 1.45 ± 0.06, and thymocyte density decreased from 12,450 ± 420 to 10,320 ± 380 cells/mm². Hassall's corpuscle diameter increased from 38.6 ± 1.4 to 52.8 ± 1.9 μm.

At 9 months, the cortical proportion decreased from 61.7 ± 1.7% in controls to 48.5 ± 1.5% in the experimental group, and the medullary proportion increased from 38.3 ± 1.7% to 51.5 ± 1.5%. The corticomedullary ratio decreased from 1.61 ± 0.07 to 0.94 ± 0.05. Thymocyte density fell from 10,980 ± 360 to 8,240 ± 310 cells/mm², whereas Hassall's corpuscle diameter increased from 45.3 ± 1.6 to 67.5 ± 2.3 μm. The source dissertation marks these experimental-versus-control differences as statistically significant at $p < 0.05$; the exact test and comparison basis should be confirmed in the original statistical output.

3.5. Collagen-positive area in the thymus

Van Gieson staining showed an increase in thymic collagen-positive area after experimental stimulation. At 4 months, the reported area increased from 1.7% in controls to 7.6% in the experimental group; at 9 months, it increased from 2.6% to 9.8%. This pattern is consistent with increased stromal collagen deposition in the experimental groups. Because the reported percentages are not accompanied by dispersion estimates, they are presented descriptively.

3.6. Thymic immunohistochemical findings

Table 3. Thymic morphometric parameters in age-matched control and experimental rats (M ± m). *The dissertation reports $p < 0.05$; the precise comparison and test should be verified against the original statistical output.

Parameter	Age	Control	Experimental
Cortical area (%)	4 months	68.4 ± 1.8	59.2 ± 1.6*
Medullary area (%)	4 months	31.6 ± 1.8	40.8 ± 1.6*
Corticomedullary ratio	4 months	2.16 ± 0.08	1.45 ± 0.06*
Thymocyte density (cells/mm²)	4 months	12,450 ± 420	10,320 ± 380*
Hassall's corpuscle diameter (μm)	4 months	38.6 ± 1.4	52.8 ± 1.9*
Cortical area (%)	9 months	61.7 ± 1.7	48.5 ± 1.5*
Medullary area (%)	9 months	38.3 ± 1.7	51.5 ± 1.5*
Corticomedullary ratio	9 months	1.61 ± 0.07	0.94 ± 0.05*
Thymocyte density (cells/mm²)	9 months	10,980 ± 360	8,240 ± 310*
Hassall's corpuscle diameter (μm)	9 months	45.3 ± 1.6	67.5 ± 2.3*

Discussion

The present analysis describes age-dependent structural responses of the spleen and thymus following experimental stimulation with a mycobacterial antigen-containing adjuvant. The two organs showed distinct but complementary patterns: splenic white-pulp representation and selected lymphoid structures increased, whereas thymic cortical representation and thymocyte density decreased. The combination of these findings indicates that the response was not uniform across lymphoid organs and should be interpreted in relation to their different anatomical and functional roles.

In the spleen, the increased white-pulp proportion, larger lymphoid follicles, thicker periarteriolar lymphoid sheaths, and increased central artery diameter are consistent with remodeling of lymphoid and vascular compartments. The concurrent increase in collagen-positive area suggests that stromal changes accompanied the altered compartment proportions. These observations are broadly compatible with the established role of the spleen in systemic antigen surveillance and immune-cell organization [2,5,6]. Nevertheless, morphometric enlargement alone cannot establish whether a response is protective, dysregulated, or functionally effective.

The thymic findings were characterized by a lower cortical proportion, a higher medullary proportion, a reduced corticomedullary ratio, and lower thymocyte density. These differences were more pronounced in the 9-month experimental group than in the 4-month group. The increased diameter of Hassall's corpuscles and higher collagen-positive area further indicate stromal remodeling. Age-associated thymic involution is well recognized [1,3,4]; therefore, the age-matched comparisons are essential, and the present data suggest an additional experimental effect beyond the descriptive differences observed between ages. However, a formal age-by-treatment interaction would be required to quantify whether age statistically modifies the response.

The splenic immunohistochemical data showed lower reported CD3- and CD20-associated percentages and higher CD68-associated percentages in the experimental groups. This pattern may reflect a shift in the relative representation of lymphocyte-associated and macrophage-associated reactions, but the denominator used for each percentage has not yet been defined in the manuscript. The thymic caspase-3 and CD138 values also varied between age groups; however, without matched control values and confirmation of whether the values are image-level or group-level estimates, these results cannot support a strong mechanistic claim. Immunohistochemical markers should be interpreted in the context of staining specificity, tissue localization, and the quantification method [7–9,15].

Digital image analysis can improve the transparency and reproducibility of morphometric measurements when images are calibrated, regions of interest are defined consistently, and thresholds and sampling procedures are reported [10–17]. QuPath v0.5.1 was used in the present workflow. This should be described as software-assisted digital pathology unless a separately validated artificial-intelligence model, including training data, reference annotations, and performance metrics, was actually developed. The distinction is important because software-assisted quantification does not by itself demonstrate the validity of an AI classifier [11,12,16–18].

Several limitations should be considered. The exact number of animals allocated to each age and condition, details of the administration protocol, antibody specifications, image-sampling plan, and the denominators used for immunohistochemical percentages were not available for the present analysis. Some immunohistochemical values lack dispersion estimates, and the exact statistical tests and p-values are not provided. These limitations restrict replication and the strength of inferential conclusions.

Conclusion

Experimental mycobacterial-antigen stimulation was associated with measurable remodeling of both the spleen and thymus in rats, with patterns differing by organ and age.

In the spleen, the reported findings included an increased white-pulp proportion, enlargement of selected lymphoid and vascular structures, increased collagen-positive area, lower reported CD3- and CD20-associated percentages, and higher CD68-associated percentages.

In the thymus, the experimental groups showed reduced cortical representation and thymocyte density, an increased medullary proportion and Hassall's corpuscle diameter, and increased collagen-positive area. These changes were more pronounced in the 9-month group in the reported morphometric comparisons.

Digital image-assisted morphometry provided quantitative descriptions of the tissue changes. The findings should be interpreted in light of the experimental design and the methodological limitations described above.

The authors declare no conflict of interest.

Acknowledgments
Funding Source

Data Availability Statement

Conflicts of Interest
The authors declare no conflict of interest. [Confirm this declaration with all authors.]

Compliance with Ethical Standards

References
1. Pearse G. Normal structure, function and histology of the thymus. Toxicologic Pathology. 2006;34(5):504–514. doi:10.1080/01926230600865549.
2. Cesta MF. Normal structure, function, and histology of the spleen. Toxicologic Pathology. 2006;34(5):455–465. doi:10.1080/01926230600867743.
3. Gray DH, Seach N, Ueno T, et al. Developmental kinetics, turnover, and stimulatory capacity of thymic epithelial cells. Blood. 2006;108(12):3777–3785. doi:10.1182/blood-2006-02-004531.
4. Palmer DB. The effect of age on thymic function. Frontiers in Immunology. 2013;4:316. doi:10.3389/fimmu.2013.00316.
5. Bronte V, Pittet MJ. The spleen in local and systemic regulation of immunity. Immunity. 2013;39(5):806–818. doi:10.1016/j.immuni.2013.10.010.
6. Mebius RE, Kraal G. Structure and function of the spleen. Nature Reviews Immunology. 2005;5:606–616. doi:10.1038/nri1669.
7. Kaufmann SHE. How can immunology contribute to the control of tuberculosis? Nature Reviews Immunology. 2001;1:20–30. doi:10.1038/35095558.
8. O'Garra A, Redford PS, McNab FW, Bloom CI, Wilkinson RJ, Berry MPR. The immune response in tuberculosis. Annual Review of Immunology. 2013;31:475–527. doi:10.1146/annurev-immunol-032712-095939.
9. Cooper AM. Cell-mediated immune responses in tuberculosis. Annual Review of Immunology. 2009;27:393–422. doi:10.1146/annurev.immunol.021908.132703.
10.Horai Y, Kakimoto T, Takemoto K, Tanaka M. Quantitative analysis of histopathological findings using image processing software. Journal of Toxicologic Pathology. 2017;30(4):351–358. doi:10.1293/tox.2017-0031.
11.Bankhead P. Developing image analysis methods for digital pathology. The Journal of Pathology. 2022;257(4):391–402. doi:10.1002/path.5921.
12.Madabhushi A, Lee G. Image analysis and machine learning in digital pathology: challenges and opportunities. Medical Image Analysis. 2016;33:170–175. doi:10.1016/j.media.2016.06.037.
13.Gurcan MN, Boucheron LE, Can A, Madabhushi A, Rajpoot NM, Yener B. Histopathological image analysis: a review. IEEE Reviews in Biomedical Engineering. 2009;2:147–171. doi:10.1109/RBME.2009.2034865.
14.Abels E, Pantanowitz L. Current state of the regulatory trajectory for whole slide imaging devices in the USA. Journal of Pathology Informatics. 2017;8:23. doi:10.4103/jpi.jpi_31_17.
15.Lara H, Li Z, Abels E, et al. Quantitative image analysis for tissue biomarker use: a white paper from the Digital Pathology Association. Applied Immunohistochemistry & Molecular Morphology. 2021;29(7):479–493. doi:10.1097/PAI.0000000000000930.
16.Bankhead P, Loughrey MB, Fernández JA, et al. QuPath: Open source software for digital pathology image analysis. Scientific Reports. 2017;7:16878. doi:10.1038/s41598-017-17204-5.
17.Schneider CA, Rasband WS, Eliceiri KW. NIH Image to ImageJ: 25 years of image analysis. Nature Methods. 2012;9:671–675. doi:10.1038/nmeth.2089.
18.Mehrvar S, Maisonave K, Buck W, Guffroy M, Bawa B, Himmel L. Immunohistochemistry-free enhanced histopathology of the rat spleen using deep learning. Toxicologic Pathology. 2025;53(1):83–94. doi:10.1177/01926233241303907.
19.Sun Y, et al. Exploring multiplex immunohistochemistry techniques and histopathology image analysis: current practice and potential for clinical incorporation. Cancer Medicine. 2025;14(1). doi:10.1002/cam4.70523.
20.Teshaev SJ, Qodirov OO‘, Davlatov SS, Rakhmanov KE, Hamroyev IS, Rajabova NK. Morphometric and histological alterations in the spleen induced by chronic carbon monoxide exposure and the corrective effects of Gulimaxsar. Natural and Engineering Sciences. 2026;11(2):111–116. doi:10.28978/nesciences.262009. Available from: https://nesciences.com/article/73190/

21.Kosimov UU, Turniyozov AA, Bakhronov JD, Teshaev US, Khidirov ZE, Qodirov OO‘. Morphometric, histopathological, and immunohistochemical evaluation of myocardial remodeling in cisplatin-induced renal failure in rats. Natural and Engineering Sciences. 2026;11(3):132–141. doi:10.28978/nesciences.263012. Available from: https://nesciences.com/article-category/3/